

University of Twente

EEMCS / Electrical Engineering
Control Engineering

**DESIGN OF A FLEXIBLE NEEDLE
INSERTION DEVICE WITH SYNCHRONOUS
ULTRASOUND IMAGING OF TARGET**

ing. T.R. Kerkhof

Pre-Master Individual Assignment

Committee

dr. S. Misra
M. Abayazid, MSc
dr. ir. J.F. Broenink

Januari 2012

Report nr 002CE2012
Control Engineering
EE-Math-CS
University of Twente
P.O. Box 217
7500 AE Enschede
The Netherlands

Summary

Robotic insertion of flexible needles could potentially be used to navigate the needle precisely to the target, thereby avoiding obstacles. A setup is designed to insert a flexible needle in a gel while rotating it, care is taken to minimize buckling. The insertion motion will be provided by a linear actuator powered by a servo motor, while the rotating motion is powered directly by a servo motor. These motors are controlled via a motion controller connected to a PC while an ultrasound transducer is positioned on the gel. Forces, torques and ultrasound images can be acquired and logged. The effects of buckling on the needle are studied under various circumstances and a solution is presented to avoid buckling.

Table of Contents

Abstract	4
1. Introduction	5
2. Design	6
2.1. Linear Motion	6
2.2. Rotary Motion	8
2.3. Force/Torque Sensor	10
2.4. Needle Support	11
2.5. Needle	14
2.6. Ultrasound Head Placement Device	15
2.7. Data Acquisition	16
2.8. Controller Interface	16
2.8. Final Design	17
3. Comparison With Existing Setup	19
4. Validation	20
4.1 Buckling Analysis	20
4.2 Sheath Performance	25
4.3 Ultrasound Measurements	30
4.4 Needle Steering	30
5. Conclusions and Recommendations	31
Bibliography	32

Abstract

Many modern clinical practices involve percutaneous diagnosis and therapy, in which for instance a needle is inserted into soft tissue. The precision of diagnosis and the effectiveness of therapy highly depend on the accuracy of needle placement. However, targeting accuracy is complicated by several factors, such as obstacles (anatomical constraints), tissue deformations, needle-tissue interactions, and physiological processes (e.g. breathing). Robotically steerable flexible needles offer a possible means to precisely guide the needle to a specific location along a curved path. In addition, ultrasound imaging can be used to track tumour motions and needle position during the insertion procedure.

For my pre-master individual assignment, I will design an experimental setup in which a flexible needle can be robotically inserted into a tissue-like gel including an artificial tumour. The device can accurately translate and rotate the needle tip inside the gel. Due to the flexibility of the needle, the needle can travel along a curved path, thereby avoiding obstacles. Forces and torques on the needle will be measured using a load cell attached to the base of the needle. Tumour motion and needle position will be imaged with a commercial ultrasound system. The ultrasound images will be collected simultaneous with needle base displacement and force / torque measurements by using the s-video output of the ultrasound system. Modelling, tracking and image-guided control of the flexible needle will be part of a different project, and is not part of this assignment.

The needle insertion system needs to be versatile, such that needles of different diameters and lengths could be easily attached and detached. The gel phantom is placed on a small platform attached to the linear stage that drives the needle into the gel phantom. This phantom mimics a breast with tumour and will be approximately 15 cm x 15 cm x 5 cm (width x length x height). It contains a stiffer inclusion of ~1 cm diameter to simulate the tumour. A flexible nitinol wire of ~1,0 mm diameter will be used. The needle insertion system will have a linear velocity range of 1 to 20 mm/s and angular velocity of 1 to 15 RPM. I will choose the required controller interface to accurately drive the needle into the breast phantom; any software design falls outside the scope of this project. The system will be transportable such that it can be taken to the ultrasound lab of our collaborators in Nijmegen.

1. Introduction

When a needle travels through soft tissue, the bevel tip will cause the tissue to be pushed in a certain direction. As a consequence the needle tip will experience a force in the opposite direction.

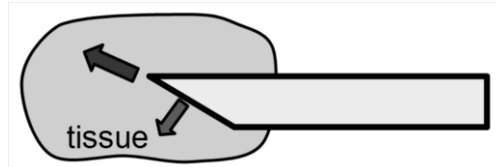


Figure 1. Force exerted on an asymmetric needle tip, Alterovitz et al, 2005

If the needle is flexible enough this force will cause it to bend and follow a curved path through the tissue. It can then be rotated to change the direction of the needle tip. This allows a target to be reached even if it is obscured by obstacles.

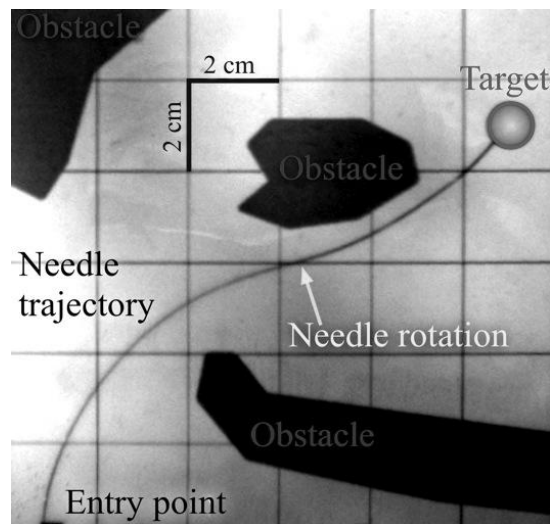


Figure 2. Example of needle steering, Reed et al, 2004

2. Design

The following chapter describes the design choices that were made during the development of the needle insertion device.

2.1. Linear Motion

To insert the needle into the phantom, a linear motion is needed. A friction drive was considered; this drive utilizes a clamping force to grasp the needle on the barrel. This grasping could be implemented using rubber rollers. An example is given in the following figure.

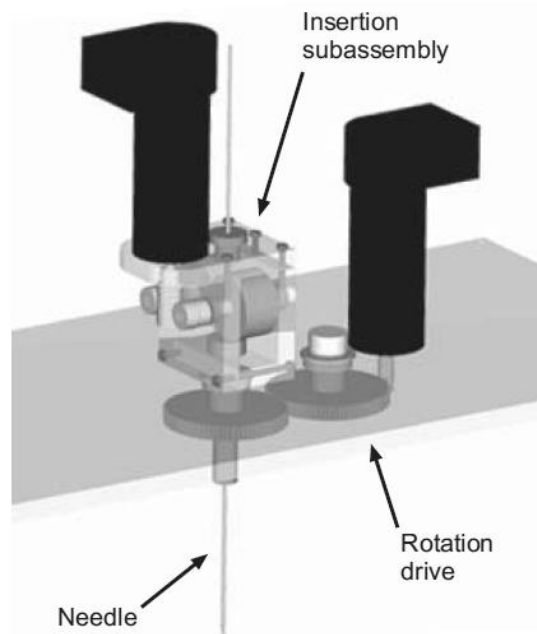


Figure 3. Example of a friction drive needle insertion, Webster et al, 2005

This design was not chosen because the slip between the rollers and the needle would cause grave inaccuracies in measuring the position and orientation of the needle. Also, the slip would lead to undesired rotation of the needle. Furthermore forces and torques on the needle would be difficult to measure.

Instead a mechanical linear actuator was chosen. This type of drive uses a rotary motor to drive a lead screw, which in turn moves a slide back and forth. Attached to this slide is the rotation drive.

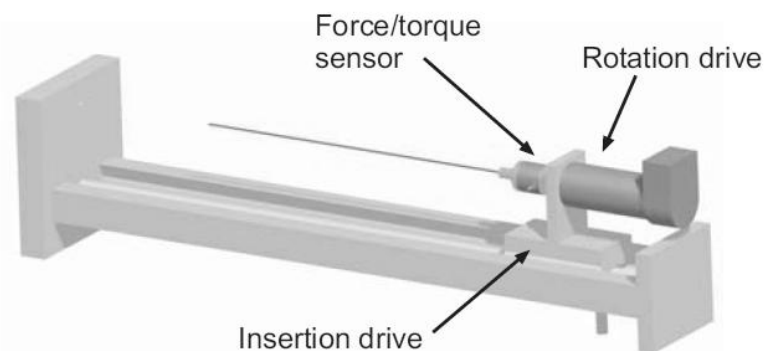


Figure 4. Example of a linear actuator needle insertion, Webster et al, 2005

A suitable model is the Misumi LX26. This linear stage provides a stroke length of 207 mm, a positioning accuracy of 0,06 mm and a maximum translation speed of 290 mms^{-1} .

The maximum velocity with which the needle will be inserted is 20 mms^{-1} , this speed will be reached in $0,20 \text{ s}$, the spindle lead is 2 mm , spindle inertia $0,0198 \text{ kgcm}^2$, mass to be accelerated $0,25 \text{ kg}$. Previous research (O'Leary et al 2003, Okamura et al 2004, Podder et al 2005, DiMaio and Salcudean 2003) suggests forces in the range of 1 N and torques of around 10 mNm , so a maximum friction force of 5 N is assumed. Because of the spindle lead of 2 mm an insertion speed of 20 mms^{-1} translates to a rotational speed of 600 rpm .

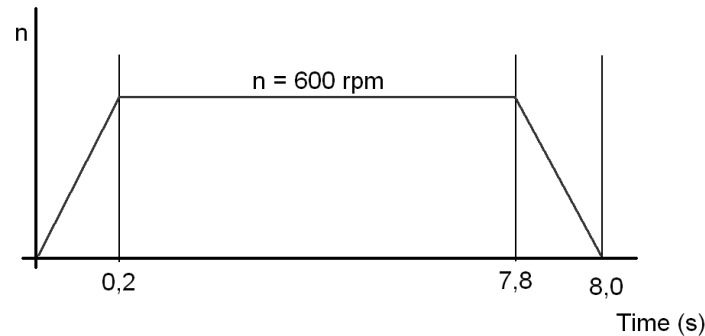


Figure 5. Rotary speed profile

The torque while accelerating is determined by the inertia of the spindle (J) times its angular acceleration (α), and the force that the phantom exerts on the needle (F_{load}). This last term can be split up in the linear inertia of the load (m_{load}) and the force the gel exerts on the needle (F_r). In formula:

$$M = J_{spindle} \cdot \alpha + \frac{F_{load} \cdot p}{2\pi} = J_{spindle} \cdot \frac{\pi}{30} \frac{\Delta n}{\Delta t} + \frac{(m_{load} \cdot a + F_r) \cdot p}{2\pi}$$

$$= 1,98 \cdot 10^{-6} \cdot \frac{\pi}{30} \frac{600}{0,2} + \frac{(0,25 \cdot 0,10 + 5) \cdot 0,002}{2\pi} = 6,2 \cdot 10^{-4} + 1,6 \cdot 10^{-3} = 2,2 \cdot 10^{-3}$$

Where p is the spindle lead.

The stall torque of the spindle drive is 20 mNm , adding to a total required torque of 22 mNm . This low torque requirement eliminates the need for a gear head. However, at the minimum speed of 30 rpm the control voltage drops significantly. Also, the resolution for position control is decreased when a gear head isn't present. The planetary gear head GP 26 B has a recommended input speed of $< 8000 \text{ rpm}$. The reduction ratio can maximally be $\frac{8000}{600} = 13,3$. The next closest is $4,4:1$ (model nr.

144027)

Because of its low cost and good controllability, a brushed motor is advantageous. However, due to the relative low speed graphite brushes will deteriorate quickly. Precious metal brushes are required. A good choice would be the Maxon RE 25, which has a nominal torque of around 25 mNm . High-ohmic windings will increase controllability because of the motor's lower speed constant, therefore model nr 118746 is selected. A suitable encoder is the Maxon HEDL 5540 with 3 mm shaft diameter, model nr 110512.

This setup was tested by modelling the system in 20-Sim.

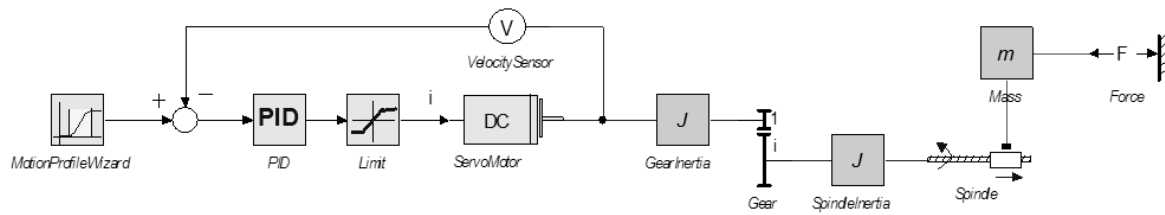


Figure 6. IPM of the translation stage

Figure 6 shows the motion profile, a simple controller, a current limiter, the servo motor, non-ideal gear with inertia, spindle with inertia, mass and constant (friction) force. A simulation was run to see if the end effector could follow the provided motion profile (figure 5).

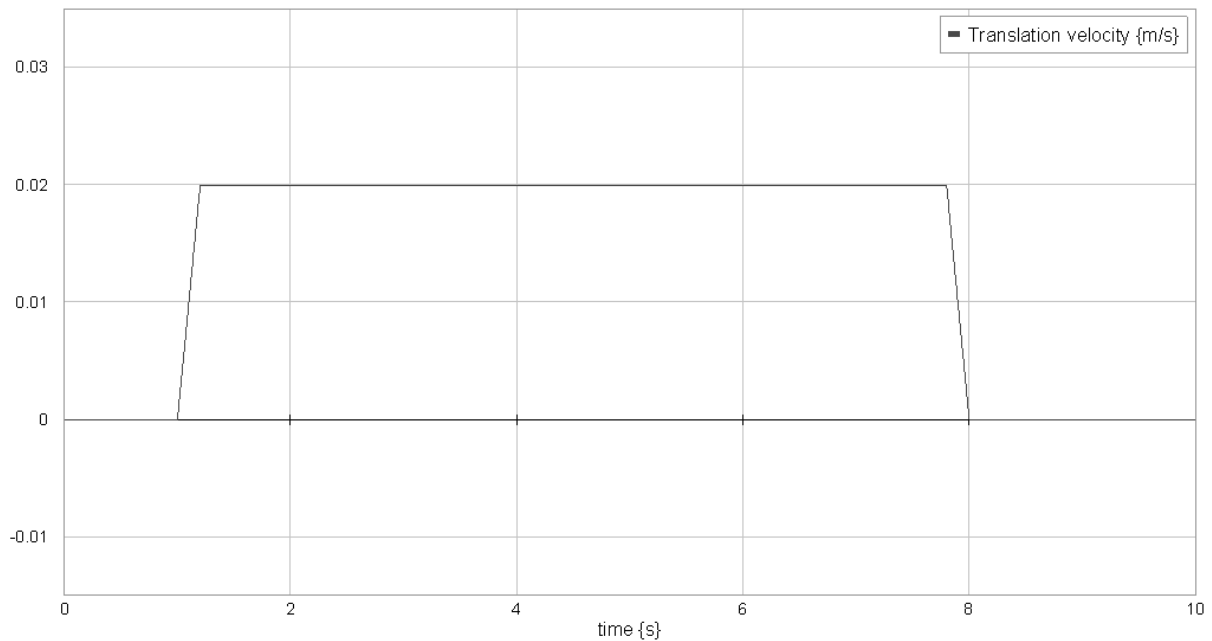


Figure 7. Simulation results showing translation speed of end effector

The simulation shows that the above described components can accelerate the mass to the desired speed of 20 mms^{-1} within the required time.

2.2. Rotary Motion

The expected peak torque for the rotary motion will be around 10 mNm. A gear is required with a maximum continuous torque of 10 mNm, but it should also be strong enough to carry the load of the force sensor, needle, etc.

One option would be the spur gear head GS 16 V, which has a recommended input speed of < 8000 rpm. This gives a reduction ratio of max 533:1. The nearest smaller ratio is 261:1 (model nr 235076). The corresponding motor would be the RE 16, also with high-ohmic windings (model nr 320178). A suitable encoder is the MR type M with 512 CPT, model nr 201937.

Again this configuration is tested by modelling it.

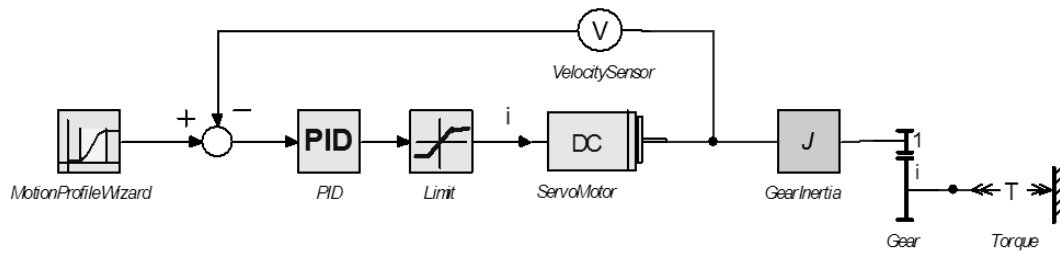


Figure 8. IPM of the rotation stage

Figure 8 shows the motion profile, a simple controller, a current limiter, the servo motor, non-ideal gear with inertia and constant (friction) torque. The inertia of the needle is neglectable. A simulation was run to see if this system is able to rotate the needle at the required speed .

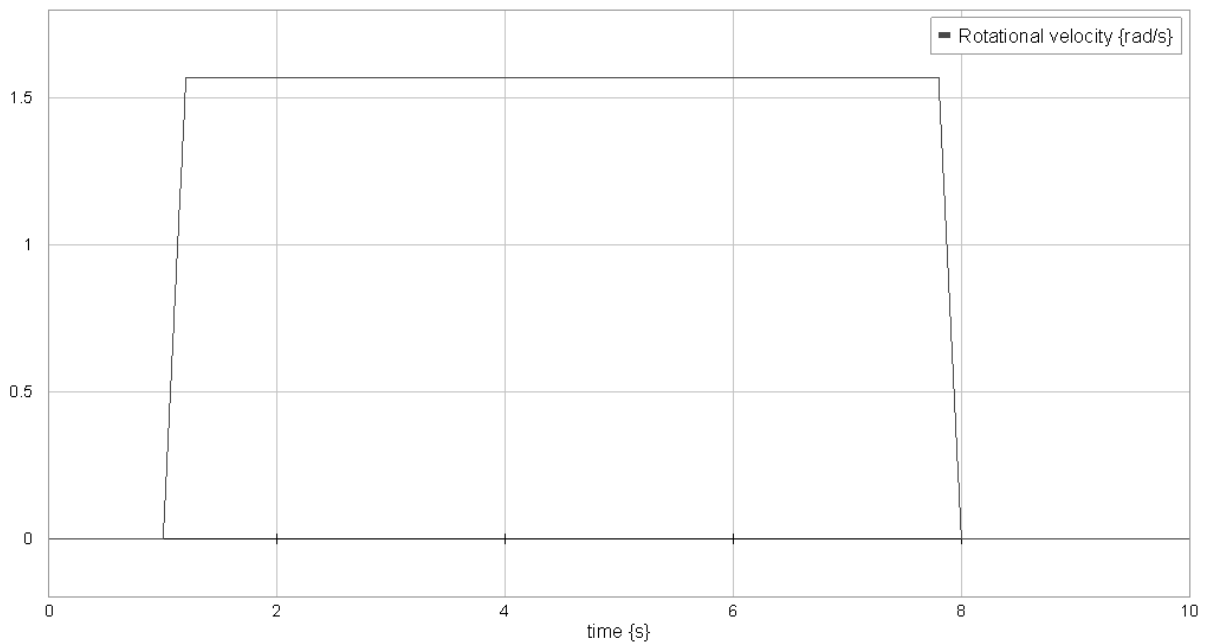


Figure 9. Simulation results showing rotation speed of end effector

The simulation shows the selected components are able to accelerate the needle to 15 RPM within 0.2 seconds.

To attach the motor to the linear drive a mechanical part need to be machined. This component should be strong enough to repeatedly perform consistent insertions, easily disassemblable and preferably made from sheet material. The final design consists of three pieces which are machined from 10 mm sheet aluminium to save on material and labour cost. Aluminium also doesn't corrode and can be easily sterilised. The pieces are joined by bolts to allow for simple disassembly.

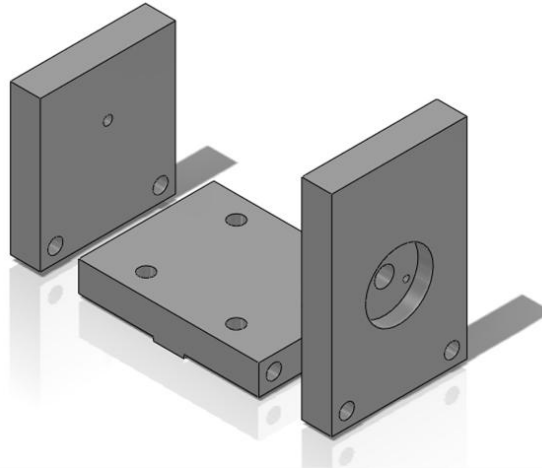


Figure 10. Rotary motor adapter parts.

2.3. Force/Torque Sensor

The force/torque sensor can be placed in a number of places in the system, as shown in the figure below.

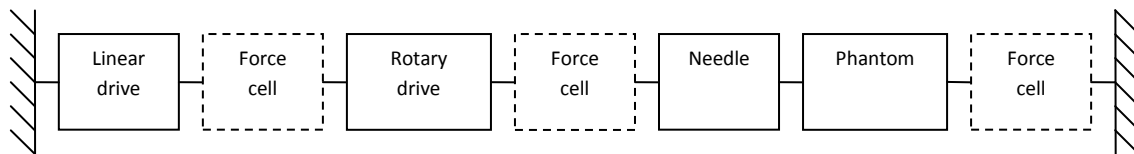


Figure 11. Possible locations for force measurement.

Because both the torques and the forces on the needle are of interest, the best place to attach the load cell would be at the base of the needle. This will cause the load cell cable to get tangled up after a few rotations, but because of the low rotation speed this doesn't have to be a problem.

Because the force and torque on the needle are expected to be relatively small, measuring range and resolution are key aspects. The following table shows a comparison of two frequently used force/torque sensor systems.

	ATI Nano17	JR3 20E12
Full scale force (z-axis)	17 N	40 N
Force resolution	1/320 N	1/200 N
Full scale torque	120 mNm	1000 mNm
Torque resolution	1/64 mNm	1/8 mNm
Price	6199 \$	6445 \$

Because of its superior specifications and lower price, the Nano17 is chosen.

2.4. Needle Support

The needle used will be made of an ultra-flexible alloy. Because of its flexibility the needle is inclined to buckle when axial force is applied. When this happens the needle doesn't form a straight line anymore which could make it impossible to insert the needle at all. To prevent this, a support structure will be made. Although the buckling is worse near the insertion the needle has to be supported along its entire length, yet the support should have minimum effect on the force / torque measurements. Several options are researched.

Firstly a sabot-type construction is considered, where a semi-rigid shell surrounding the needle is attached to the rotation subassembly. When the shell reaches the phantom it parts from the needle to allow unperturbed insertion.

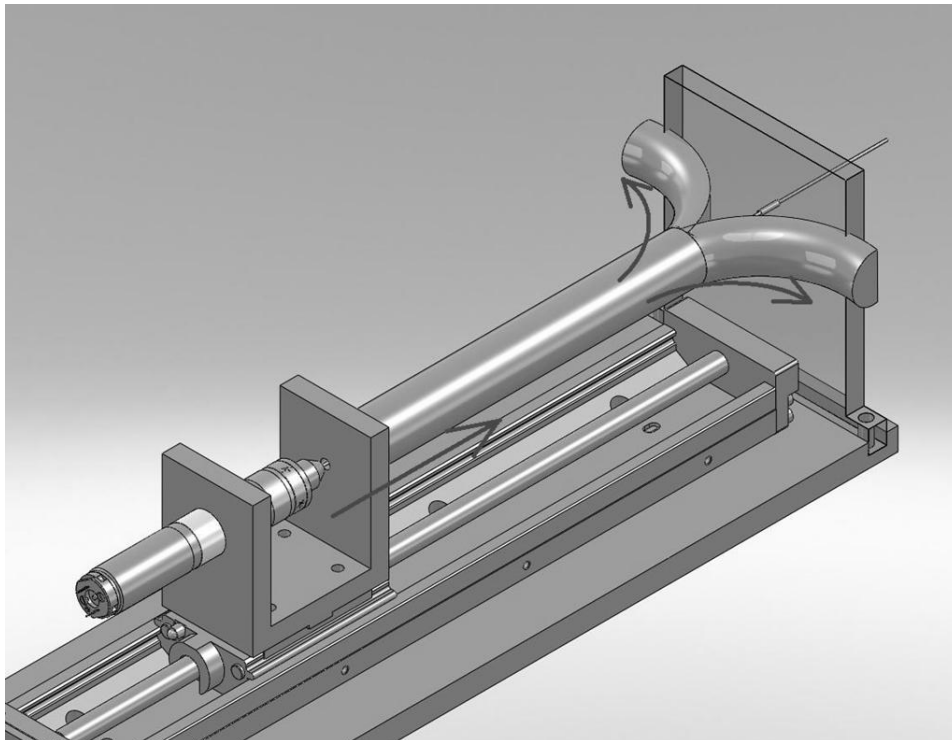


Figure 12. The rigid sabot separates from the needle as it is inserted

Depending on the implementation the sabot can be single use only or it can be reused for multiple insertions. An advantage of such a setup is that the needle will be supported along its entire. A downside is that the design of the sabot is very difficult; it has to be rigid enough to prevent the needle from buckling but flexible enough to part from the needle at the right moment.

Another option is to attach a number of supporting struts to the sides of the base plate. These struts will be pushed to the side by the moving rotation subassembly, thus only supporting the needle where needed.

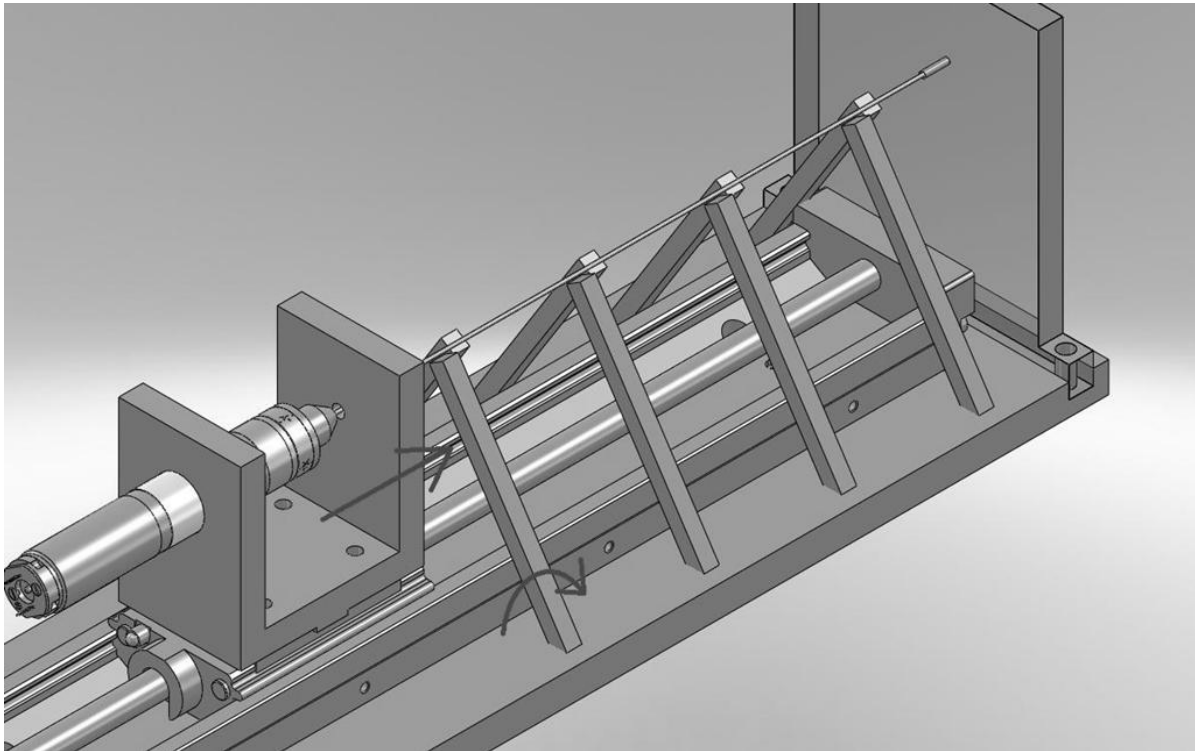


Figure 13. Needle supported by struts. As the rotation subassembly moves forward the struts are pushed out of the way

Using this method the contact area between needle and support is very small; therefore friction forces disturbing the measurements will also be small. This solution however is mechanically very complex and has to be manually reset after each insertion. Also the needle is only supported at certain points.

Finally a telescopic sheath could be implemented. This is a segmented, rigid, hollow tube which surrounds the needle. Each segment is slightly smaller in diameter than the previous; as the needle is inserted the segments slide over each other. The sections should be sufficiently small so that the maximum insertion depth should still be achieved.

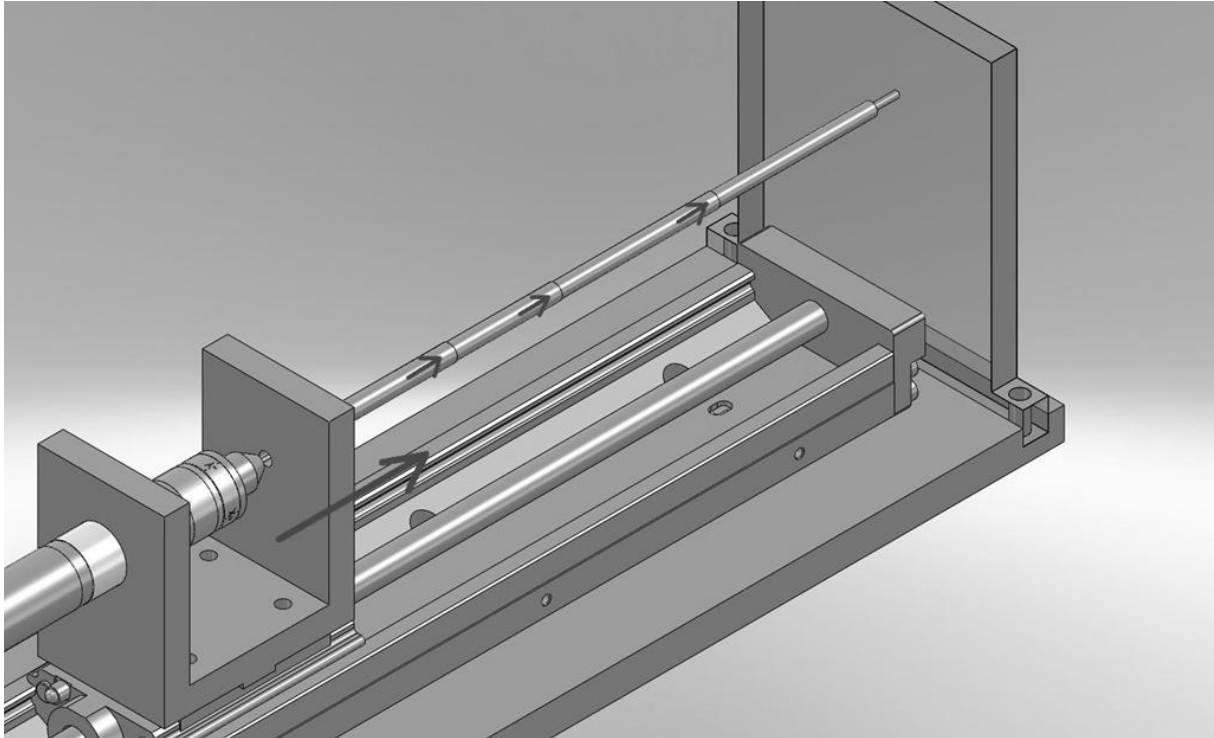


Figure 14. As the needle is inserted the sheath sections slide inside one another

This solution is cheap and mechanically simple while providing excellent support, which is why it is eventually chosen.

In order not to negatively influence the stroke length the sheath segments should be as small as possible. However, each additional segment introduces unwanted flexibility in the sheath. A compromise is found at a segment length of 50 mm; this allow for a maximum stroke length of 190 mm while retaining overall rigidity.

The above proposed buckling prevention method introduces additional forces due to the contact between the needle and the sheath; this compromises the reliability of measurements. This effect could be cancelled out if the contact forces between the needle and the sheath were measured. It is chosen not to do this because in practise this is virtually impossible and because these forces will be significantly smaller than the needle insertion forces.

At the widest end the sheath has an internal screw thread. This will be used to fix the sheath to the motor bracket by first screwing a hollow bolt in the bracket. This bolt will protrude a few millimetres, the sheath is subsequently screwed onto the protruding hollow bolt. The needle will be inserted through the bolt and into the sheath.

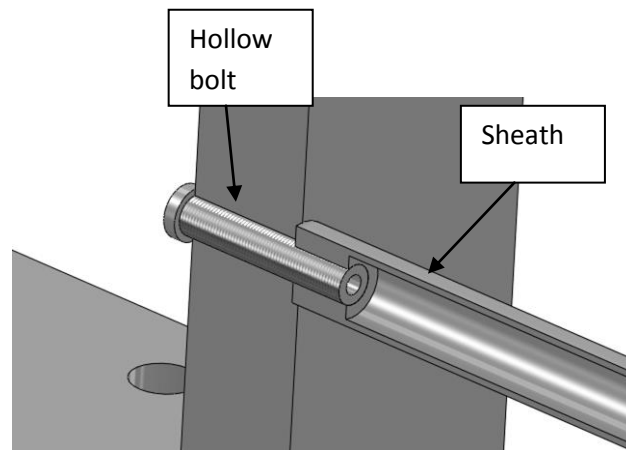


Figure 15. Section view of how the sheath is attached to the rotation subassembly.

The other end of the sheath is fixed to a plastic plug which can be inserted in an acrylic end plate. Acrylic is chosen because it allows for a better view of the need insertion. The plug can be clicked into the acrylic plate after which the sheath can be secured to it using a small bolt.

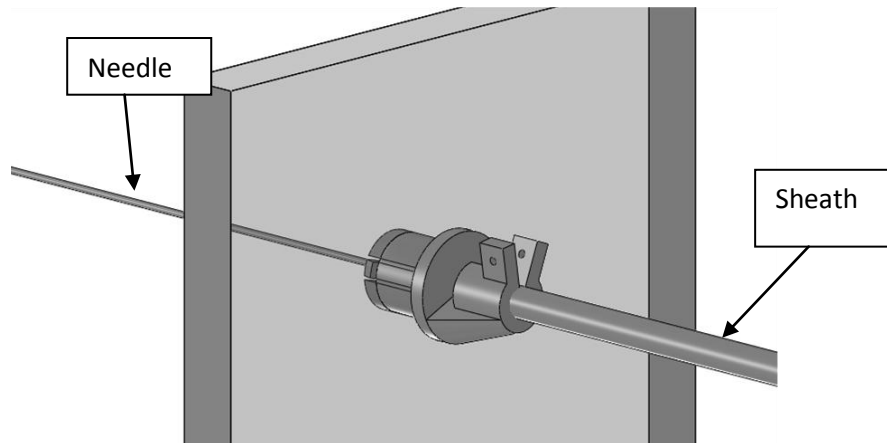


Figure 16. Plug which secures the sheath and guides the needle.

2.5. Needle

The material from which the needle is made is Nitinol, which is an alloy of nickel and titanium and is used for medical needles because of its exceptional biocompatibility, especially in the areas of corrosion resistance and thrombogenicity (Shabalovskaya, 2002). Another property of nitinol is superelasticity, which allows for steerable needles.

Several suppliers of this alloy exist in the Benelux, offering a range of heat- and surface treatments. After requesting a number of quotes it was decided to order several meters of four different diameters from Flexmet BVBA. The heat treatment is straight drawn and the surface treatment is centerless grinded. Next the Nitinol wire is cut to lengths of 200 mm and cast in a gel under a certain angle after which the gel is allowed to set. The tip of the needle is then shaped using a rotary sander.

2.6. Ultrasound Head Placement Device

While inserting the needle ultrasound images need to be recorded. To this end the ultrasound transducer must be hold still on top of the gel medium. Apart from holding it by hand, one option would be to manufacture a custom clamp. This would ensure a good grip, but would cost a lot of time and money to construct. An off-the-shelf solution would be sufficiently adequate. Eventually a lab stand with three-prong was chosen because of the availability and the option to clamp other types of ultrasound transducers.



Figure 17. Ultrasound head placement device.

The stand was found to be insufficiently stable, so a new steel base plate was ordered from Misumi. This component can be bolted to the optical table for enhanced stability.

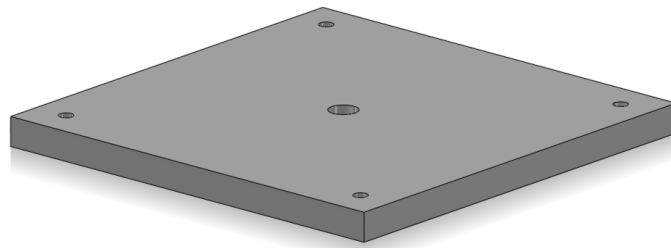


Figure 18. Base plate for ultrasound head placement device.

2.7. Data Acquisition

B-mode ultrasound images are recorded by a Siemens Acuson S2000 ultrasound system (Siemens Healthcare, Erlangen, Germany), equipped with a linear array ultrasound transducer (18L6). The image acquisition takes place in Matlab; to do this the Mathworks Image Acquisition Toolbox is needed. Supported hardware includes industrial grade image acquisition cards, which are very expensive, and generic USB interfaces. The ultrasound machine has an s-video output, which means that using a USB video grabber the images can be read into Matlab.



Figure 19. Siemens Acuson S2000 ultrasound system.

The force/torque sensor is connected to a proprietary interface board which in turn sends signals to a NI PCIe-6320 X-Series DAQ card (National Instruments Corporation, Austin, U.S.) These signals are also read into the Matlab program.

2.8. Controller Interface

The motion controller generates set points and closes the position and/or velocity feedback loop. The choice was made to use the Elmo Whistle (Elmo Motion Control, Petach-Tikva, Israel). This controller is commonly used within the University of Twente, is controlled digitally, can control current, velocity and position, and supplies up to 20 ampere, which is more than enough current. Data will be fed to the motion controller from a PC running Matlab.

2.8. Final Design

Below is the final design of the device.

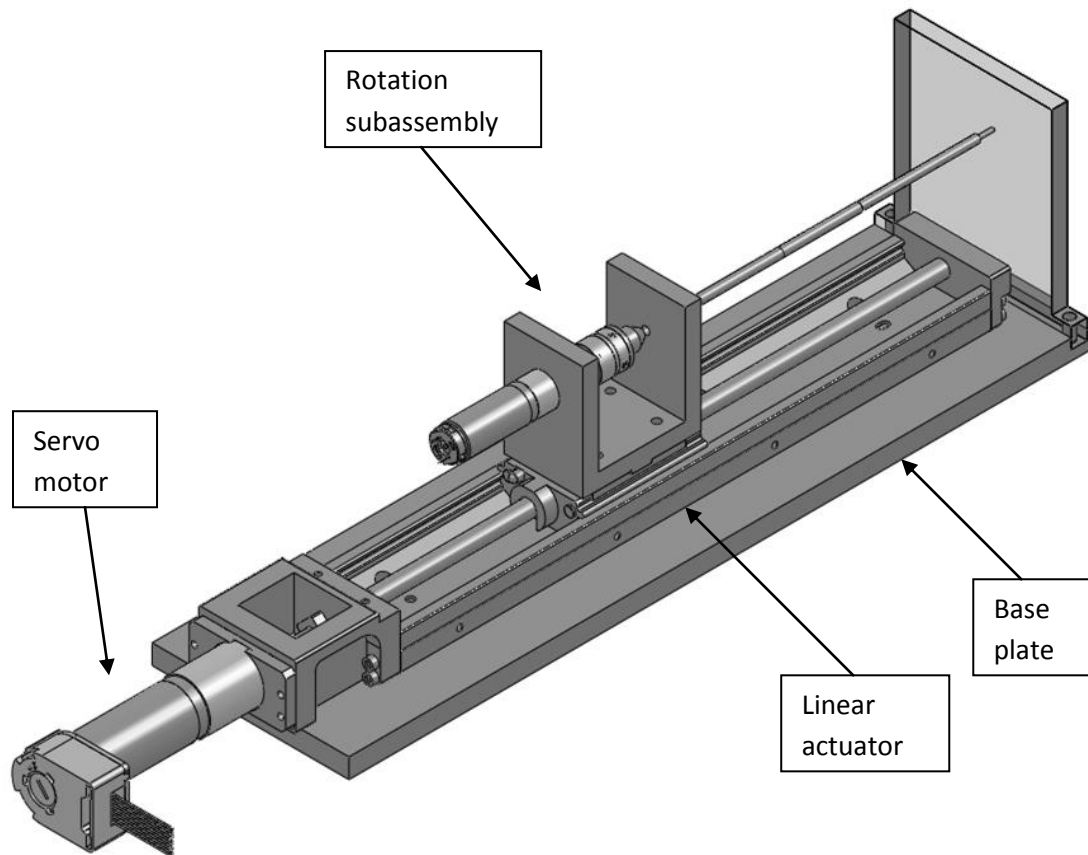


Figure 20. Final design overview.

The rotary motor is fixed to an aluminium bracket which also contains the force/torque sensor and collet/chuck to hold the needle. Also attached to this bracket is the needle support sheath.

The device is portable in the sense that the entire assembly is fixed to a base plate, allowing it to be transported without having to disconnect every component. This decreases wear and ensures correct alignment. Once disconnected from the optical table the setup is light and small enough to be carried in a briefcase or similar. Once on site the wires can be hooked up again.

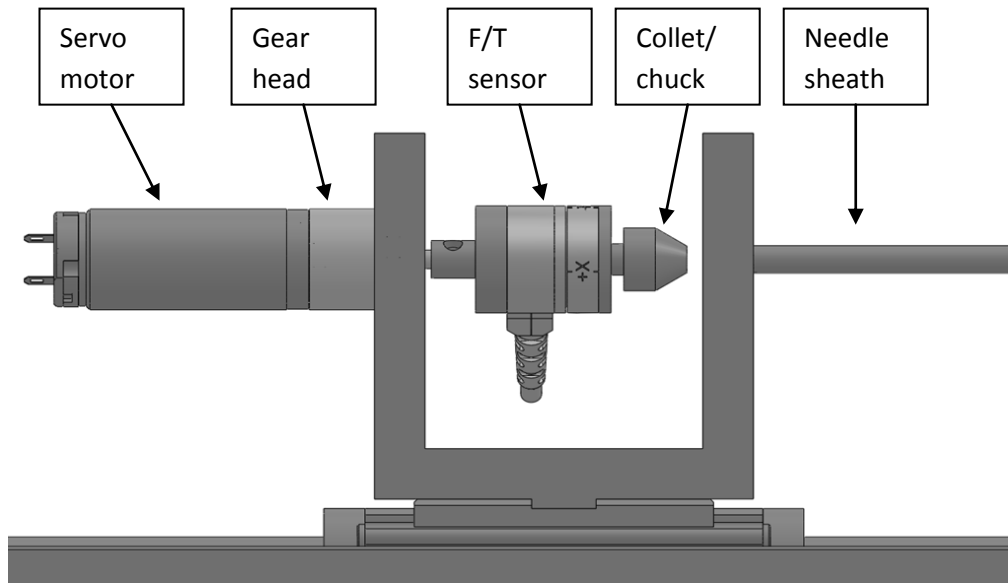


Figure 21. Final design rotation subassembly.

The other end of the sheath is mounted to a transparent plate, which allows an unobstructed view of the phantom.

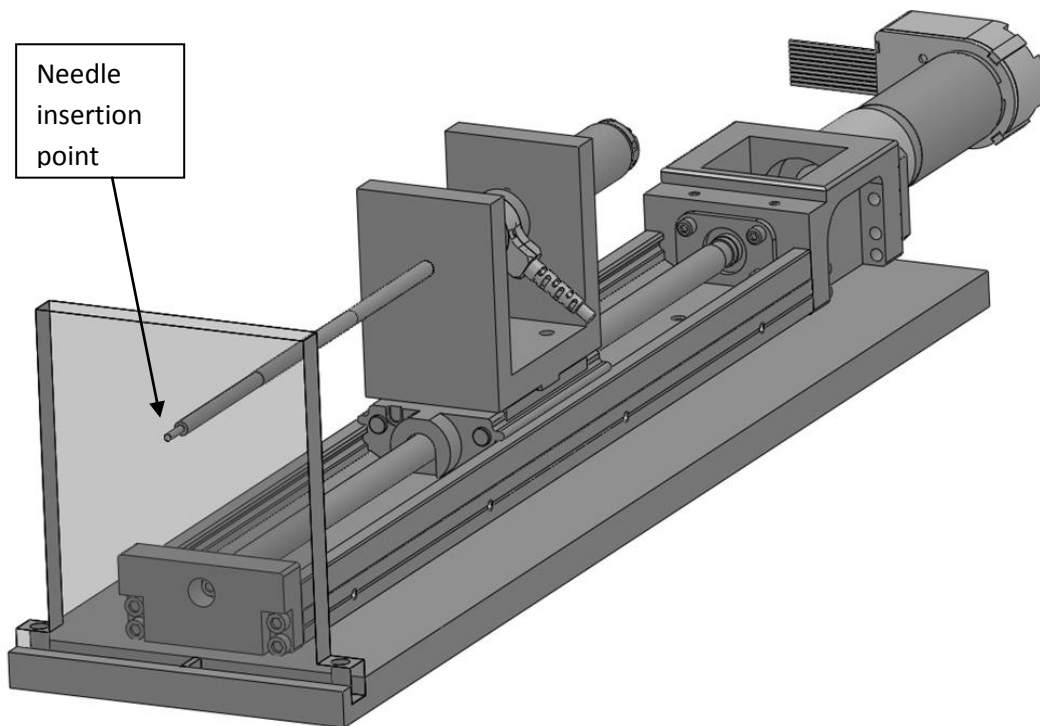


Figure 22. Final design insertion point detail.

3. Comparison With Existing Setup

A mechanical needle insertion system already exists at the University of Twente which is able to insert a needle into a soft tissue simulant (gel). The following is an abstract from Van Veen: The system can accurately translate and rotate the needle tip within the gel. The system is capable of force measurements of the needle. This is accomplished by using a load cell on the base of the needle and other novel methods of force measurement (e.g. Fiber Bragg grating sensors, microsensors etc.) which can be implemented along the shaft of the needle or at the tip. The needle path is tracked using a camera system. Tracking the tip of the needle will be used in other experiments in which image-feedback is necessary to accurately control the position of the tip.

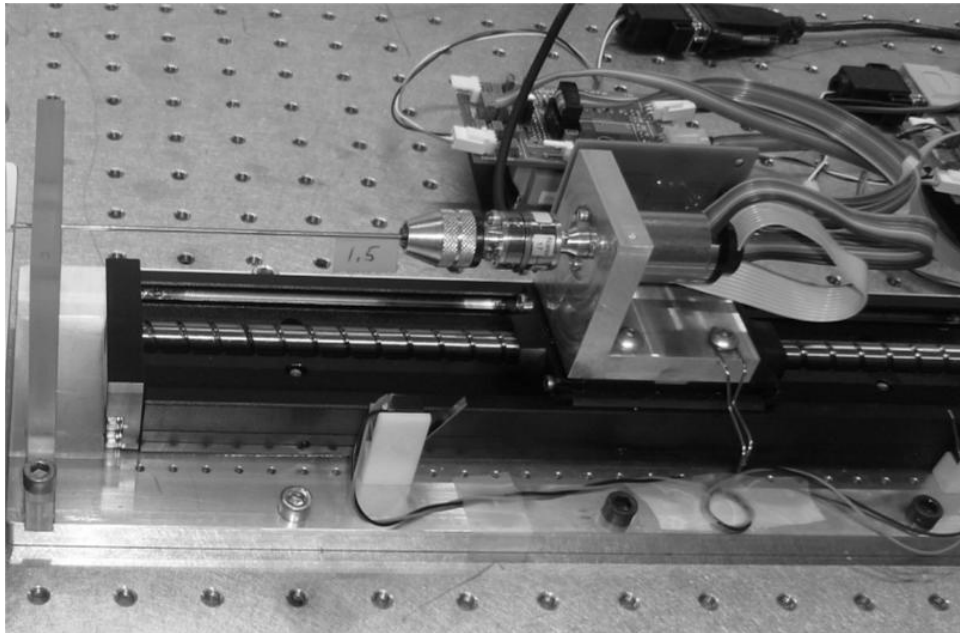


Figure 23. Rotation subassembly and needle insertion drive of existing setup.

A number of significant differences exist between the existing device and the design proposed in this report; most importantly (the lack of) a buckling prevention solution. When thinner and more flexible needles would be inserted they would buckle under the axial forces. With the proposed design buckling of flexible needles will not occur.

Another difference between the setups is the rotation assembly. In the current device the force/torque sensor is connected directly to the motor which leads to a certain amount of play in the orientation of the needle and also means the orientation can't be accurately measured. This is because the encoder only has a limited number of "clicks" or pulses per rotation which translates to a limited resolution. In the proposed design a gear head is placed in between the two which increases accuracy and resolution. When a gear head with a reduction of 4,4 is mounted, the resolution of the encoder increases with a factor 4,4.

The translation stage of the device also differs. The existing setup has a spindle lead of 5 mm which means for every rotation of the spindle the needle moves 5 mm forwards. Again the encoder on the spindle has limited accuracy; there are a limited number of clicks for every 5 mm. The proposed device has a lead of 2 mm which means the same amount of clicks are compressed into 2 mm. This will lead to a decrease in maximum insertion speed but an improved resolution on the position measurement. Because the maximum insertion speed in both cases is far beyond the requirement, a higher resolution is preferred.

4. Validation

To proof the concept of the design the existing setup (chapter 3) is used but modified. The existing L-shaped rotary subassembly is replaced by the newly designed U-shaped subassembly. Also a telescopic sheath is fitted into the setup, however instead of the proposed 50 mm a unit is used with segments of 118 mm because of availability.

Nitinol needles with diameters of 0,8 mm and 1,0 mm with bevel tips of 30° and 45° will be inserted 60 mm into 14,9% and 20% gel media at velocities of 5, 10 and 15 mms^{-1} both with and without the sheath. Video's will be recorded during the insertions to assess the amount of buckling. In this chapter buckling is defined as the amount the needle deviates from a straight line in the horizontal plane. Because the amount of buckling in the vertical plane was minimized this is assumed to be a reasonable measure for total buckling in 3D space.

4.1 Buckling Analysis

In order to make statements about the anti-buckling solution, first buckling was researched. The effect of different factors on the amount of buckling was studied.

4.1.1 Needle Diameter

Although only two thicknesses were available conclusions can still be drawn. The smaller needle with a diameter of 0,8 mm buckles a lot more than the 1,0 mm needle in all tests. This was to be expected as the thinner a needle is the more flexible is it and thus more susceptible to buckling.

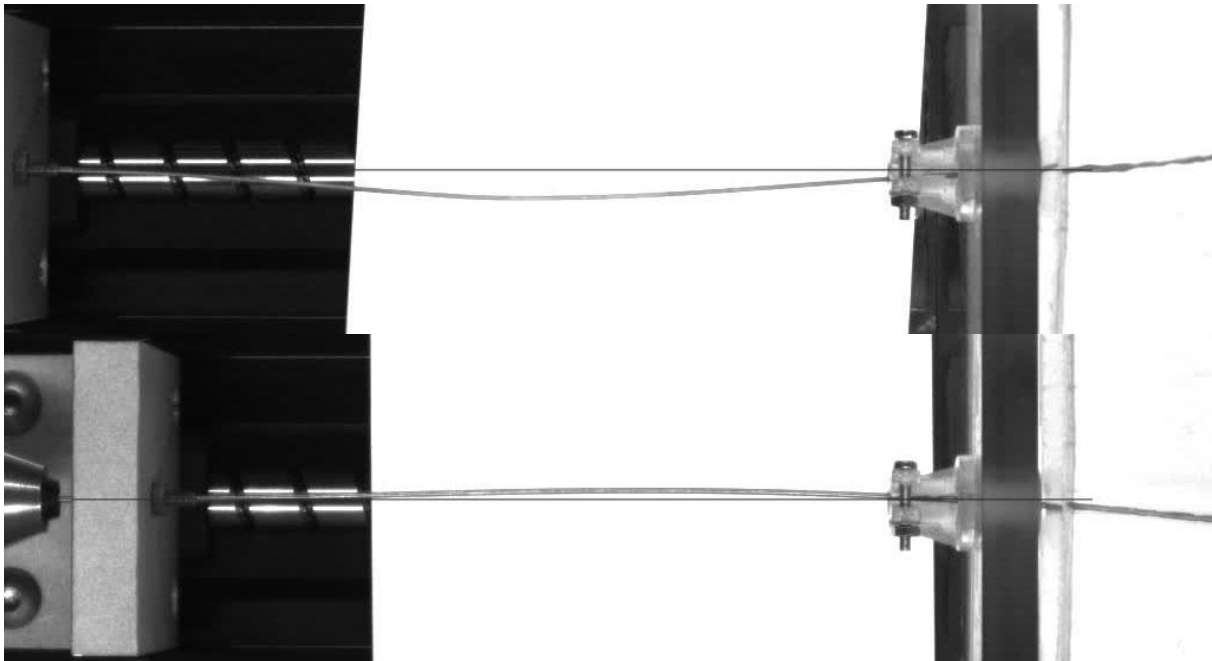


Figure 24. A 0,8 mm (above) and 1,0 mm (below) needle with a bevel angle of 45° inserted into a 14,9% gel at 5 mms^{-1} .

The force along the needle F_z is greater when a 1,0 mm needle is inserted because it deforms the gel more (note that compression force is displayed as a negative value in the graphs). Because buckling is limited the lateral force F_{xy} is also small although it is greater with the 0,8 mm needle. Although the thinner needle buckles more, torque is greater with the 1,0 mm needle. This is due to the stiffness of the thicker needle.

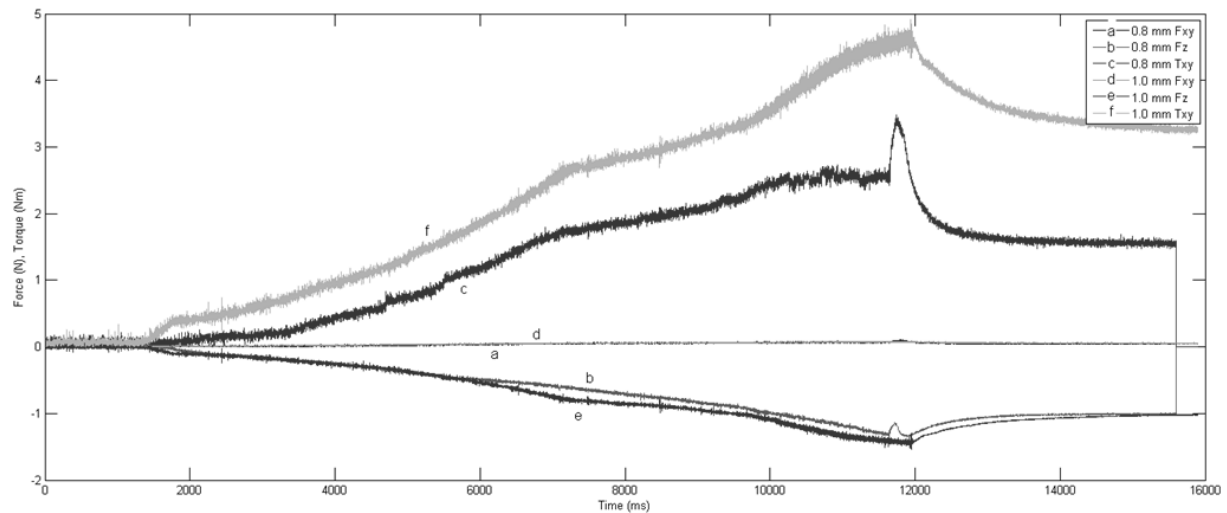


Figure 25. Force/torque graph of inserting a 0,8 and 1,0 mm needle with a bevel angle of 45° into a 14,9% gel at 5 mms^{-1} .

4.1.2 Bevel Angle

Again only two different bevel tips were available; 30° and 45° . The 45° bevel causes more buckling because it encounters greater friction in the gel.

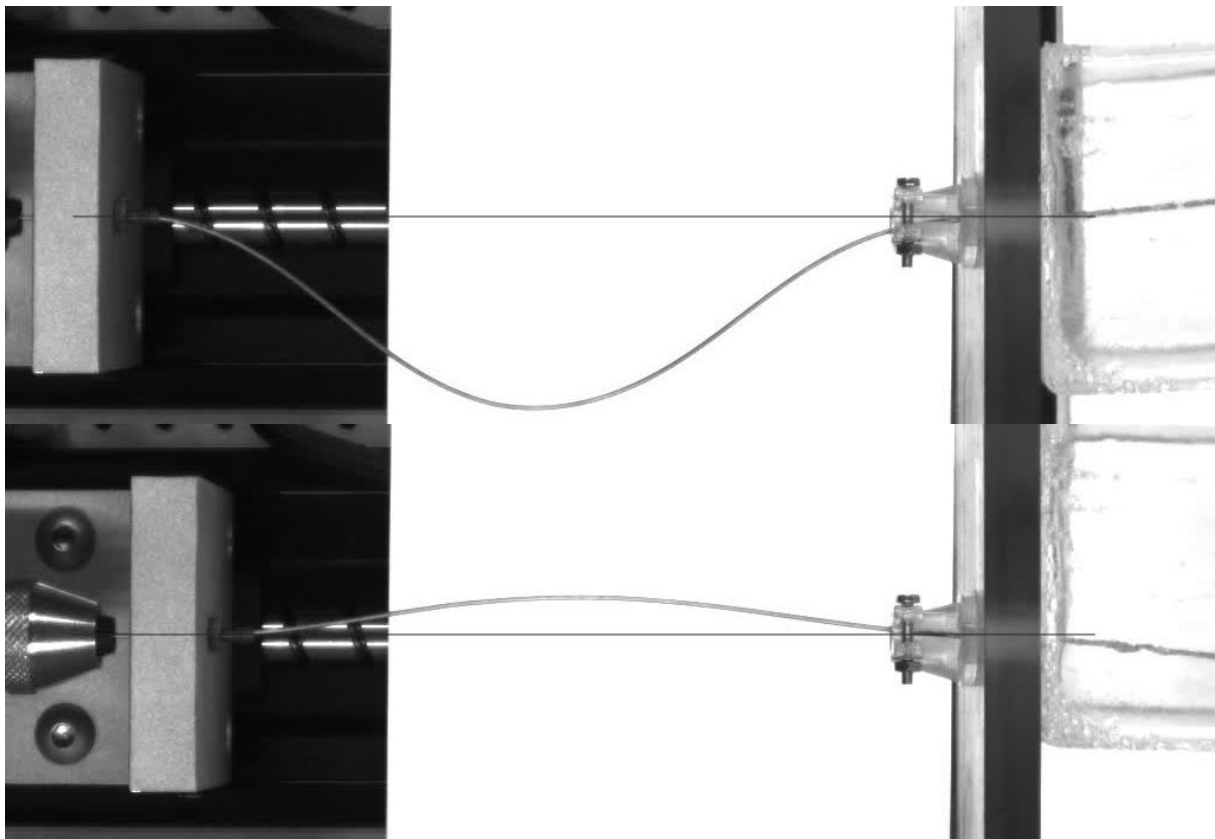


Figure 26. A 0,8 mm needle inserted into a 20% gel at 5 mms^{-1} with a bevel angle of 45° (above) and 30° (below).

The force graph shows that initially the force needed to insert the needle with a 45° bevel is greater than that needed to insert the needle with a 30° bevel. At some point the needle with a 45° bevel starts to buckle and the force along the needle decreases as the needle stops penetrating the gel. The graph becomes ever more jittery due to stiction and the torque increases due to the buckling.

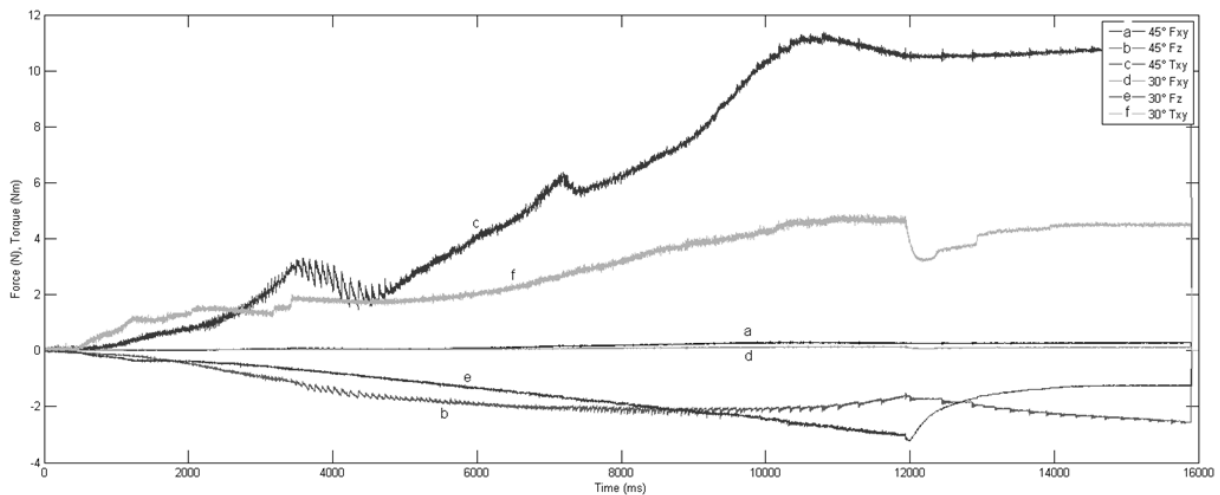


Figure 27. Force graph of inserting a 0,8 mm needle with a bevel angle of 45° and 30° into a 20% gel at 5 mm s^{-1} .

4.1.3 Gel Concentration

Two commonly used types of gel are 14,9 and 20. This means that the final tissue stimulant consists of 14,9% gelatine and 85,1% water or 20% gelatine and 80% water. The greater the relation between gelatine and water in the gel the thicker and less viscose it becomes. This would mean that a needle passing through a 20% gel would encounter more resistance than it would when passing through a 14,9% gel leading to more buckling. This was confirmed by the experimental data.

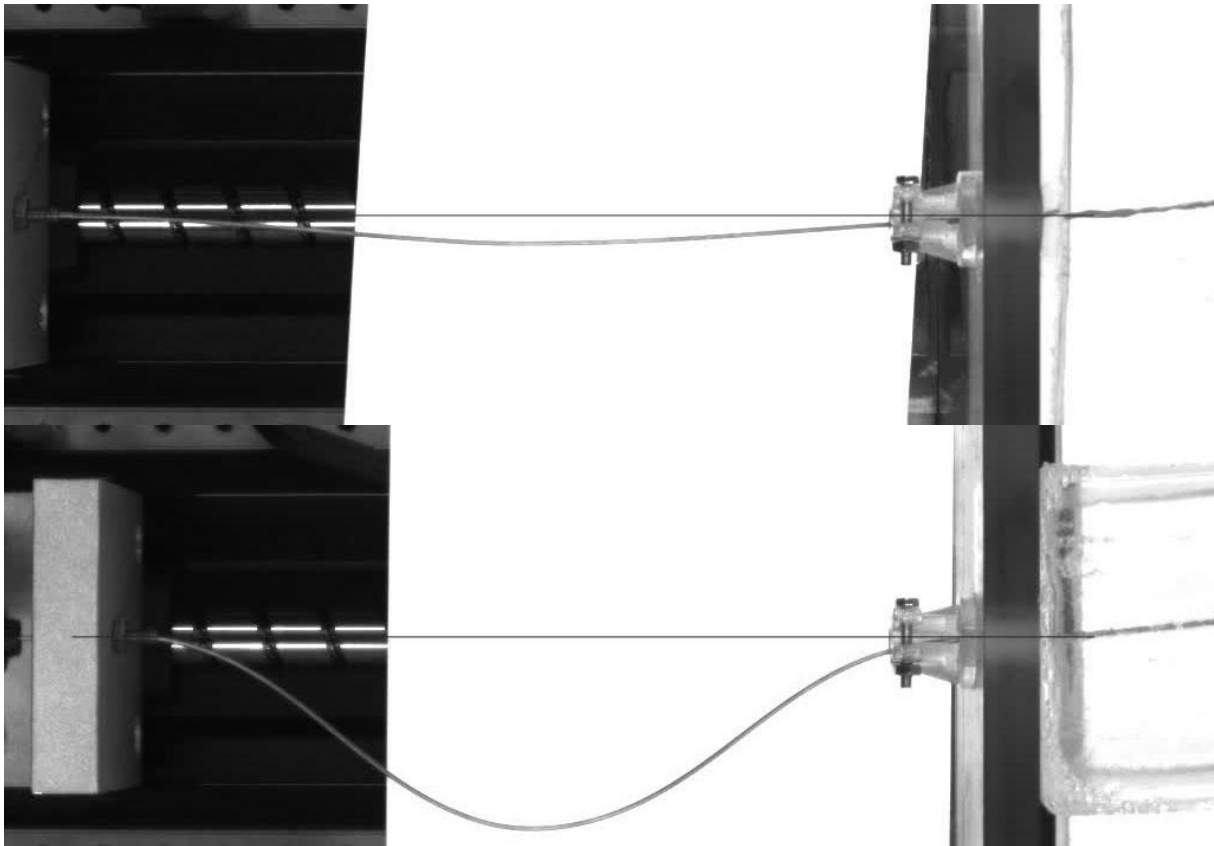


Figure 28. A 0,8 mm needle with a bevel angle of 45° inserted into a 14,9% (above) and 20% (below) gel at 10 mms^{-1} .

Initially the force on the needle is greater when it is inserted into the 20% gel. Again at some point the needle in the 20% gel starts to buckle and the force along the needle decreases as the needle stops penetrating the gel. Simultaneously the torque increases rapidly. With the 14,9% gel there is a sudden spike of torque once the needle is fully inserted. This is due to the gel springing back which would also account for the drop in axial force.

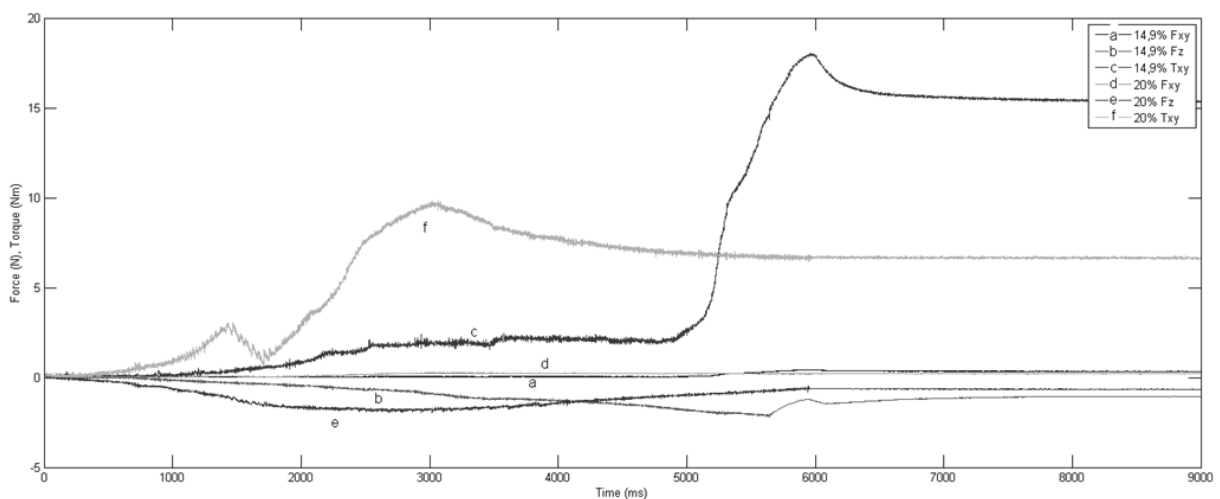


Figure 29. Force/torque graph of a 0,8 mm needle with a bevel angle of 45° inserted into a 14,9% and 20% gel at 10 mms^{-1} .

4.1.4 Insertion Speed

A needle was inserted into the gel medium at speeds of 5, 10 and 15 millimetres per second. Higher speeds seem to cause more buckling, which can be explained by the fact that the needle 'settles' in the gel after some time. If the insertion speed is higher the needle will not settle and will buckle more.

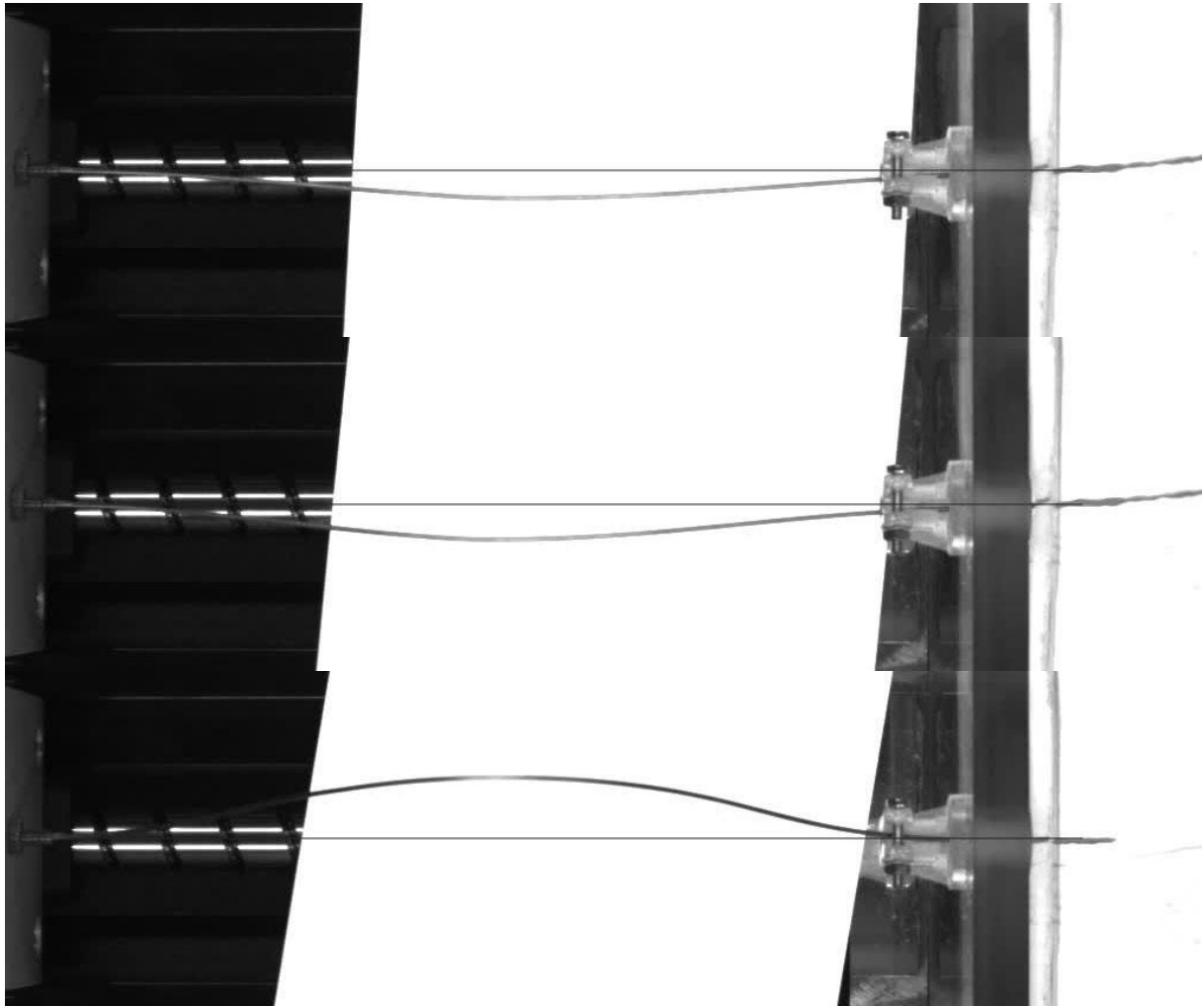


Figure 30. A 0,8 mm needle with a bevel angle of 45° inserted into a 14,9% gel at (from top to bottom) 5, 10 and 15 mm/s^{-1}

The faster the needle is inserted the greater the force along the needle. Once the needle starts buckling at 10 and 15 mm/s^{-1} the torque on the needle increases.

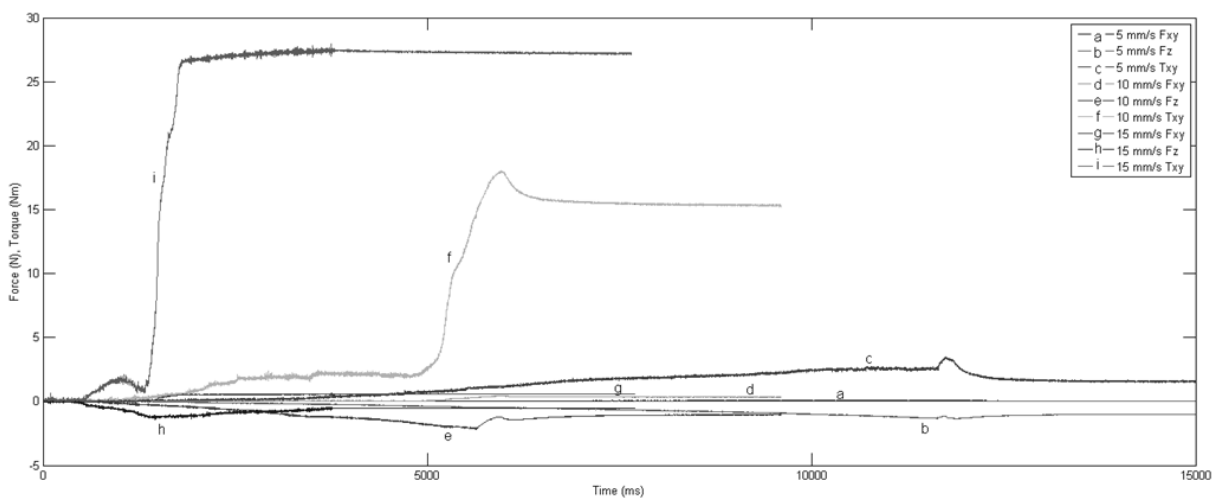


Figure 31. Force/torque graph of a 0,8 mm needle with a bevel angle of 45° inserted into a 14,9% gel at 5, 10 and 15 mm/s^{-1}

4.2 Sheath Performance

It should be noted that the experiments described above were conducted with the needle being supported near the F/T-sensor and near the insertion point; this influences the forces and torques on the needle. To research this, two needles are inserted without these supports and the forces and torques are registered.

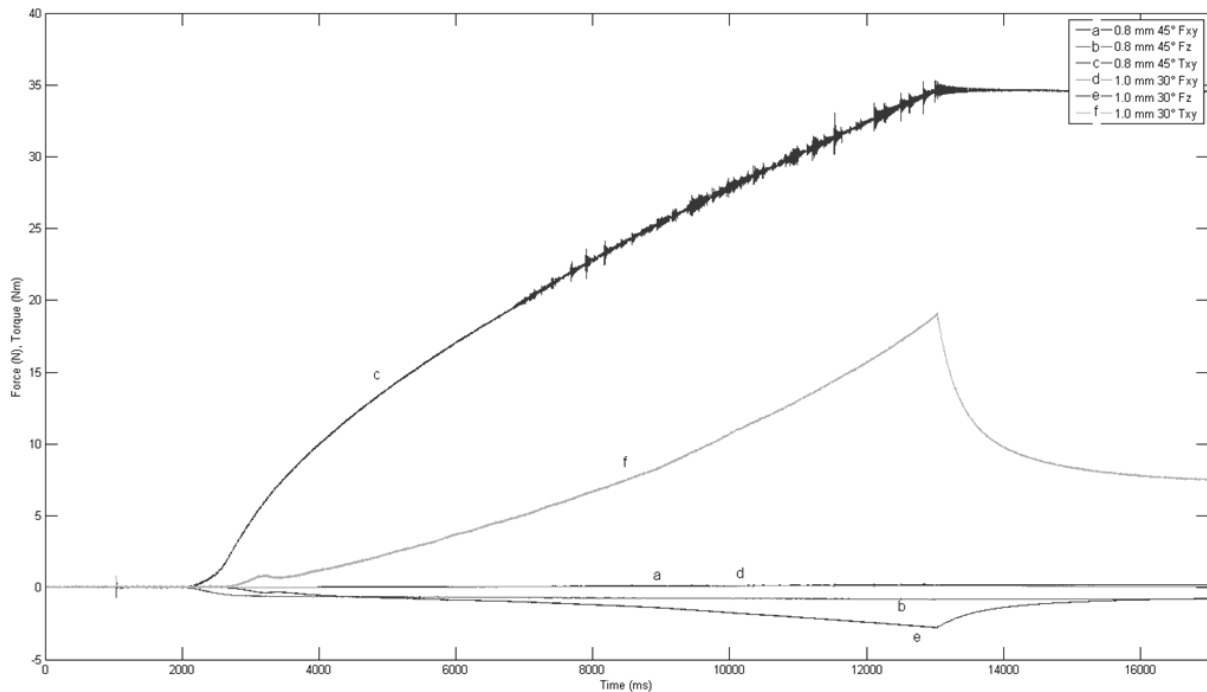


Figure 32. Force/torque graph of a 0,8 mm 45° and 1,0 mm 30° needle inserted into a 20% gel at 5 mm s^{-1} without any support

The first needle is a 0,8 mm needle with a bevel angle of 45° because this needle showed the most amount of buckling in previous tests. Again the needle buckled tremendously with great torque readings as result. The axial force increases during the first few milliseconds after insertion but then stays at the same level. The other needle is a 1,0 mm with a bevel angle of 30° because that buckled the least in previous tests. During insertion the axial force steadily increases as a result of friction inside the gel and the torque also rises due to the limited amount of buckling.

The same set of experiments was run again only now with the anti-buckling solution fitted.



Figure 33. A 0,8 mm needle with a bevel angle of 45° inserted into a 20% gel at 5 mm s^{-1} with sheath

The addition of the sheath led to significant reduction of buckling in all cases as the needle was contained within the sheath. This increases the effective insertion depth.

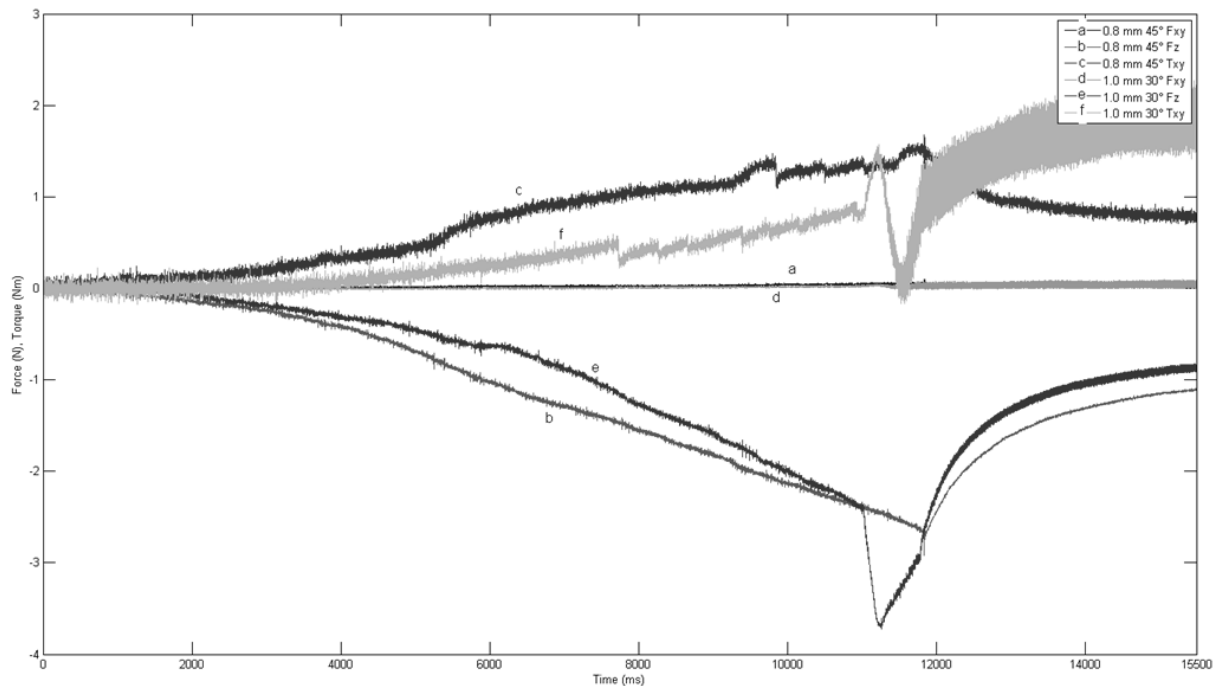


Figure 34. Force/torque graph of a 0,8 mm 45° and 1,0 mm 30° needle inserted into a 20% gel at 5 mms⁻¹ with sheath

The force graph shows a steady increase in force with both needles as resistance in the gel grows due to the deeper penetration. The torque is many times smaller compared to insertions without a sheath. This is because the needles exits the rotation subassembly in a much straighter line. It seems that with the sheath attachment more energy is directed towards inserting the needle instead of bending it. It was also observed that with the addition of the sheath the insertion still went smooth; no creaking, bending, faltering etc was detected. Below is listed the maximum amount of buckling, the maximum force along the needle and the maximum lateral torque for each variation.

Needle diameter	Bevel angle	Gel concentration	Insertion speed	Sheath			No sheath		
				Buckling (mm)	Force (N)	Torque (Nm)	Buckling (mm)	Force (N)	Torque (Nm)
0,8 mm	45°	14,9%	5 mm/s	1,0	2,19	1,23	4,2	1,39	3,57
			10 mm/s	1,0	2,71	1,32	5,2	2,18	18,08
			15 mm/s	1,0	3,10	2,03	9,1	1,4	27,97
		20%	5 mm/s	1,0	3,23	1,55	28,5	2,68	11,20
			10 mm/s	1,0	4,20	2,33	41,2	2,03	10,68
			15 mm/s	1,0	5,12	2,92	33,0	2,08	9,07
	30°	14,9%	5 mm/s	1,0	1,42	1,05	4,0	2,11	6,53
			10 mm/s	1,0	2,42	2,11	7,4	3,38	12,85
			15 mm/s	1,0	2,42	1,69	9,1	3,41	13,25
		20%	5 mm/s	1,0	5,24	2,02	5,4	3,22	4,88
			10 mm/s	1,0	5,09	2,74	11,2	4,00	11,00
			15 mm/s	1,0	5,47	2,23	35,2	2,06	13,32
1,0 mm	45°	14,9%	5 mm/s	0,8	1,71	1,38	1,4	1,54	4,88
			10 mm/s	0,8	2,41	1,33	1,5	2,12	6,69
			15 mm/s	0,8	2,61	1,31	1,5	2,06	6,47
		20%	5 mm/s	0,8	3,38	1,53	1,7	4,70	1,50
			10 mm/s	0,8	5,67	2,40	3,1	7,11	6,25
			15 mm/s	0,8	6,08	1,65	1,5	4,65	23,92
	30°	14,9%	5 mm/s	0,8	1,78	2,02	1,0	1,25	3,84
			10 mm/s	0,8	2,27	2,42	1,7	1,82	5,86
			15 mm/s	0,8	2,61	2,36	1,9	2,09	6,93
		20%	5 mm/s	0,8	4,64	1,87	1,2	3,64	2,26
			10 mm/s	0,8	5,56	2,59	1,0	3,86	3,06
			15 mm/s	0,8	4,79	1,76	1,0	4,87	2,49

Figure 35. Table showing the maximum amount of buckling, force and torque during the insertions. The amount of buckling listed in the *Sheath* column is the amount of room the needle has to move inside the sheath.

When the sheath is fitted buckling is reduced to a minimum. The average axial force on the needle is increased while the torque on the needle is decreased. This is in line with the observations that the needle is leaving the sensor in a straight line and overall insertion depth is greater.

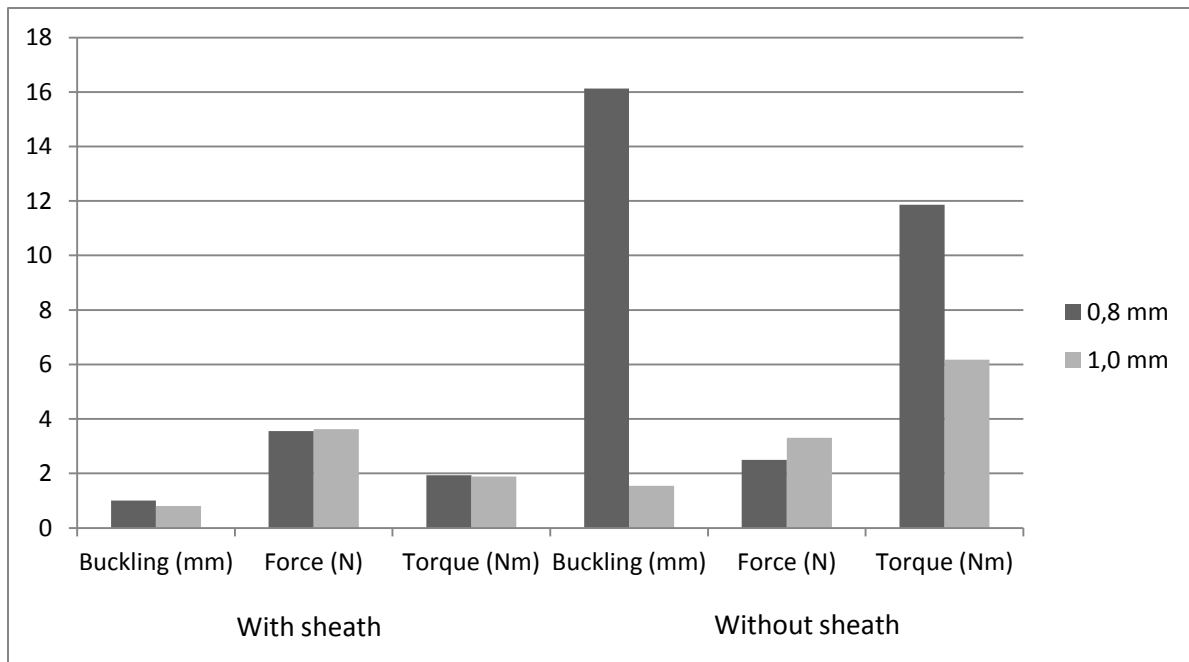


Figure 36. Graph showing the average buckling, force and torque for the 0,8 and 1,0 mm needles.

Without a sheath the 0,8 mm needles buckle a lot more than the 1,0 mm needles which leads to increased torque and decreased axial force. With sheath these values lay closer together.

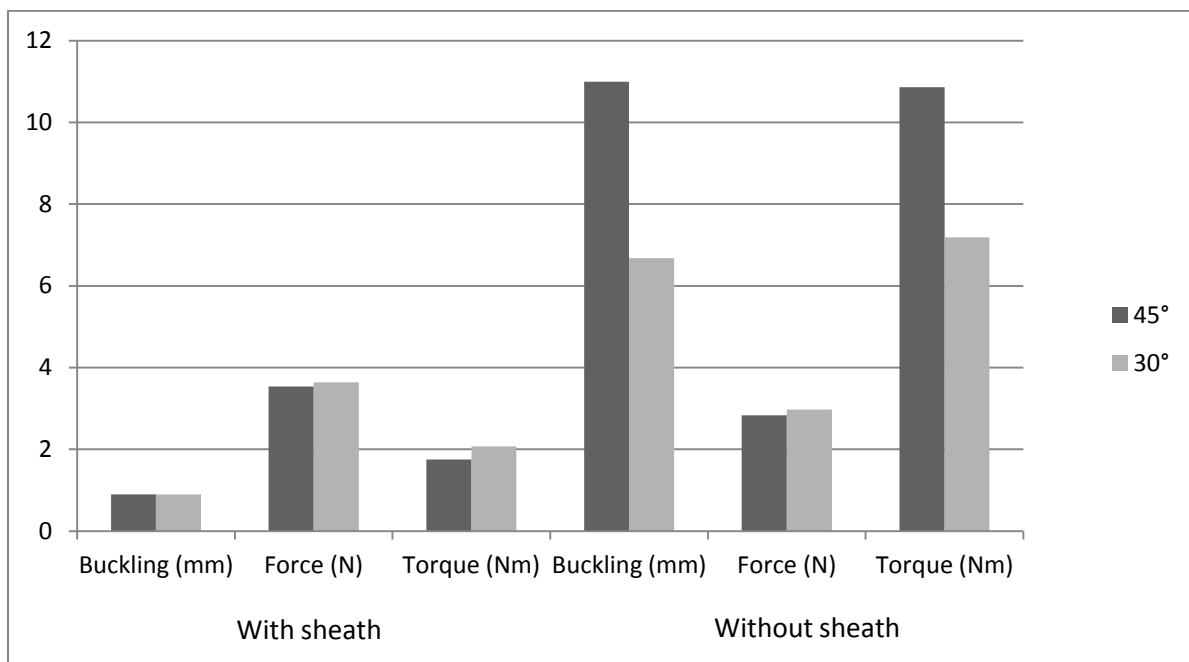


Figure 37. Graph showing the average buckling, force and torque for the 45° and 30° needles.

The 45° needles buckle a lot more than the 30° needles without sheath, which leads to increased torque and decreased axial force. With sheath the difference is much smaller.

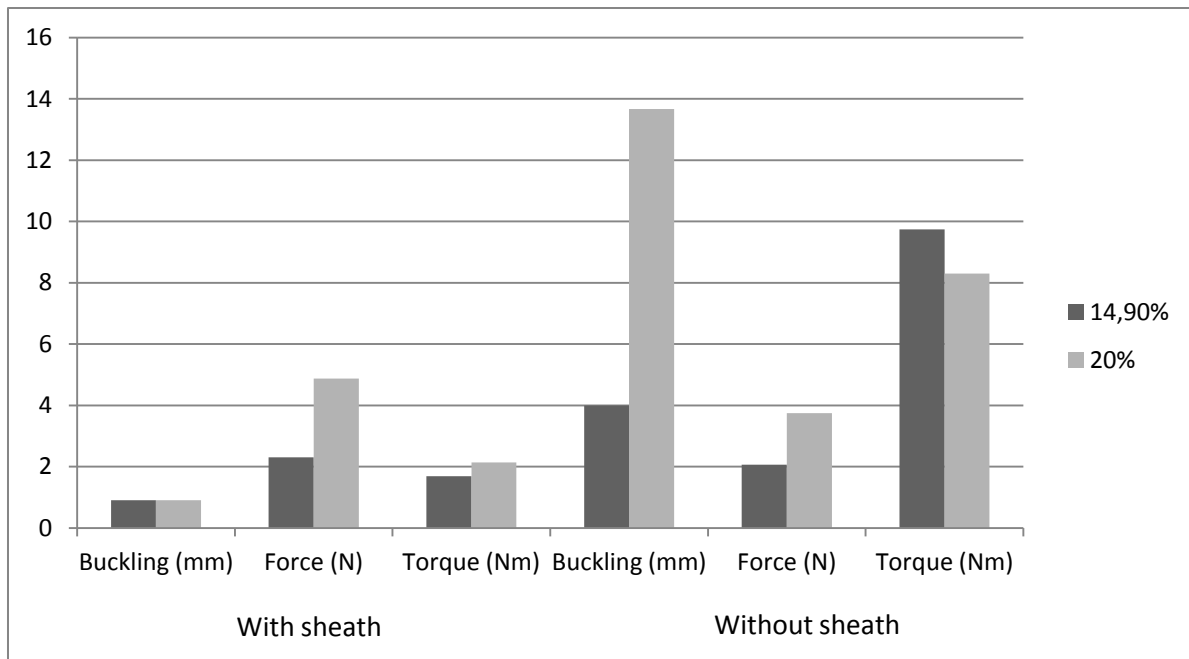


Figure 38. Graph showing the average buckling, force and torque for the 14,9% and 20% gels.

Both with and without sheath the force is greater when inserting the needle in 20% gel. Without sheath the needles buckle more with the 20% gel than with the 14,9% gel.

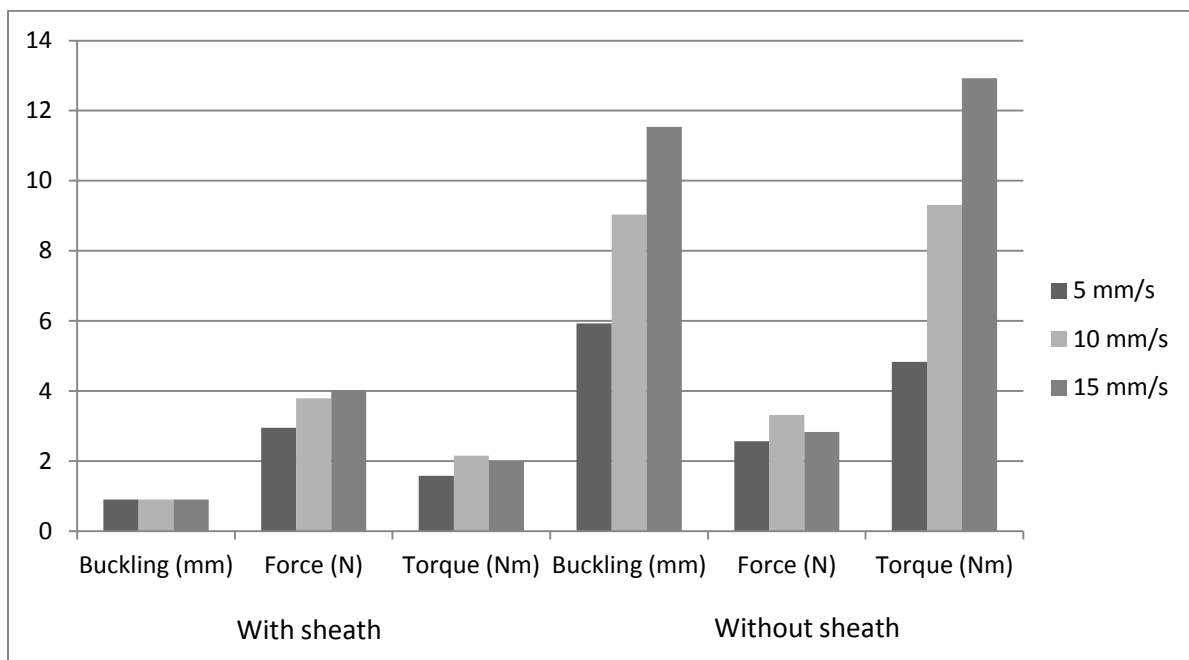


Figure 39. Graph showing the average buckling, force and torque for the 5, 10 and 15 mm/s insertion speeds.

The graph shows that the faster a needle is inserted the more it is likely to buckle which increases the torque. Very high insertion speeds require less force. Again with a sheath the values are much closer together.

As mentioned before, the sheath used in these experiments has much longer segments than proposed in the design which puts some limitations on the device. In this setup the maximum insertion depth is 12 cm, however, this requires a needle of 29 cm long. Any longer needles can't be inserted at all, while shorter needles can be inserted less deep. The minimum length a needle has to be is 17 cm.

4.3 Ultrasound Measurements

The ultrasound machine was connected to a PC using a USB video grabber.

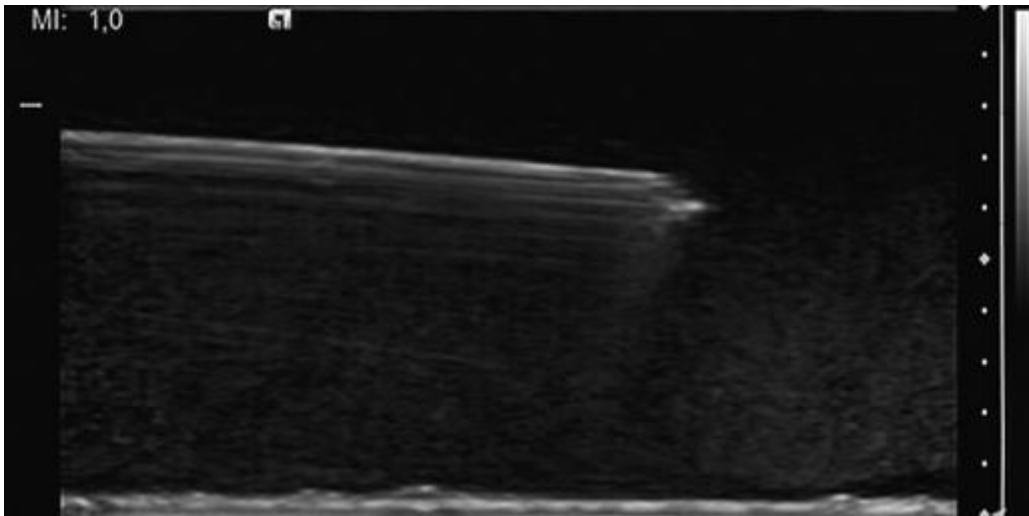


Figure 40. Ultrasound image of a needle being inserted.

During insertions the ultrasound transducer was placed on the gel using the clamp discussed earlier.

4.4 Needle Steering

To evaluate the performance of the system as a whole experiments were conducted whereby the needle had to be steered to a target while avoiding obstacles. The needle that was used has a diameter of 0,5 mm.

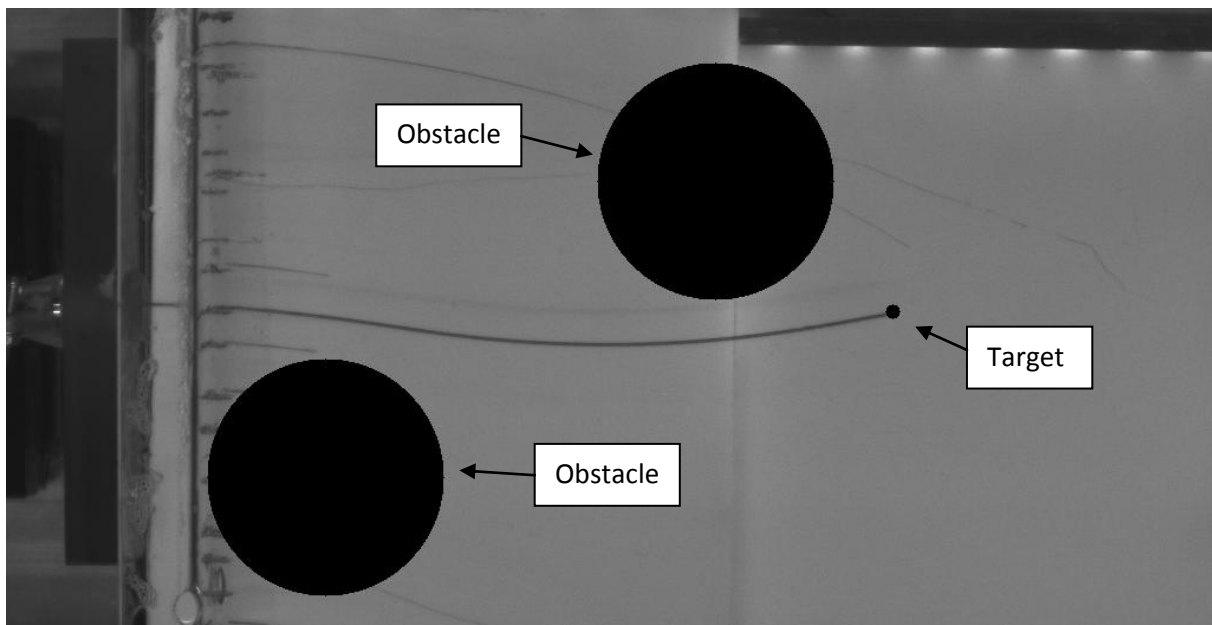


Figure 41. Flexible needle being steered around obstacles and into a target.

The device was able to successfully guide the needle tip to the target while avoiding the obstacles. Without the buckling prevention solution the needle was only able to penetrate the gel several millimetres.

Note that the above image was captured using a visible light camera because of limitations on the tissue phantom. An ultrasound imaging system would provide similar images.

5. Conclusions and Recommendations

This report has presented the design for a flexible needle insertion device with imaging of a target. The device is capable of inserting a flexible needle 15 cm with a maximum linear velocity of 20 mms^{-1} and a rotational velocity of $0,25 \text{ s}^{-1}$. It utilizes a linear slide on which a rotation assembly is fitted. Also research into buckling was done and experiments were performed.

It is shown that such a setup causes the needle to buckle when thinner needles are inserted into a tissue simulant. Analysis of the buckling behaviour of the needle shows that thinner needles, blunter bevel angles, faster insertions and denser simulant all increase buckling.

A solution to prevent the needle from flexing during insertion is to attach a segmented sheath through which the needle is inserted. This solution is tested and found to be working excellently.

Because a similar setup already exists at the University of Twente it is only needed to purchase and manufacture certain parts to convert the setup. Furthermore a method should be devised to accurately determine the orientation of the needle when fixing it in the chuck.

Bibliography

Crouch et al, "A Velocity-Dependent Model for Needle Insertion in Soft Tissue", *MICCAI 2005*, LNCS 3750, pp. 624–632, 2005

Abolhassani et al, "Trajectory Generation for Robotic Needle Insertion in Soft Tissue", *Proceedings of the 26th Annual International Conference of the IEEE EMBS San Francisco, CA, USA*, September 1-5, 2004

Webster et al, "Design Considerations for Robotic Needle Steering", *Proceedings of the 2005 IEEE International Conference on Robotics and Automation, Barcelona, Spain*, April 2005

Abolhassani et al, "Experimental study of robotic needle insertion in soft tissue", *International Congress Series 1268 (2004)* 797–802, 2004

Mahvash et al, "Mechanics of Dynamic Needle Insertion into a Biological Material", *IEEE Transactions on Biomedical Engineering*, Vol. 57, No. 4, April 2010

Meltsner et al, "Observations on rotating needle insertions using a brachytherapy robot", *Phys. Med. Biol.* 52 6027, 2007

Podder et al, "Effects of Velocity Modulation during Surgical Needle Insertion", *Proceedings of the 2005 IEEE Engineering in Medicine and Biology 27th Annual Conference Shanghai, China*, September 1-4, 2005

Bebek et al, "Design of a Small Animal Biopsy Robot", *Proceedings of the 30th Annual International Conference of the IEEE Engineering in Medicine and Biology Society, Vancouver, Canada*, August 20-24, 2008

Alterovitz et al, "Planning for Steerable Bevel-tip Needle Insertion Through 2D Soft Tissue with Obstacles", *Proceedings of the 2005 IEEE International Conference on Robotics and Automation, Barcelona, Spain*, April 2005

Shabalovskaya SA. "Surface, corrosion and biocompatibility aspects of nitinol as an implant material". *Bio-Med Mater Engin.* 2002; 12: 69-109.